DOI: 10.2352/ISSN.2470-1173.2016.9.MMRMA-361
Reprinted from
Journal of Imaging Science and Technology® 59(6): 060404-1–060404-14, 2015.

Relating Optical and Geometric Surface Characteristics for Gloss Management in Printing Applications

Teun Baar▲
Institut Mines-Télécom, Télécom ParisTech, CNRS LTCI, Paris, France
OCE Print Logic Technologies, Créteil, France
E-mail: teunbaar@gmail.com

Hans Brettel
Institut Mines-Télécom, Télécom ParisTech, CNRS LTCI, Paris, France

Maria Ortiz Segovia▲
OCE Print Logic Technologies, Créteil, France

Abstract. *There exists an increasing interest in reproducing surface appearances by means of digital printing, thereby expanding the reproduction from only color to reproduction of texture and reflection properties such as the BRDF. Previous research has focused on different ways to obtain control of the optical characteristics of digital prints, either by introducing additional inks or by modulating the surface texture on a macro level. The authors propose to utilize the different parameters of a printing system, which influence aspects such as the ink deposition and drying time, to impact the roughness of the print surface on a micro level. By investigating relationships between optical and geometric characteristics of printed surfaces, we study the hypothesis that both surface characteristics can be estimated from a single roughness parameter. From these findings, we propose a workflow to control reflection properties (including color) of a printed surface by determining ink coverage values and print parameters.*

INTRODUCTION

During recent decades, research concerning printing systems has mainly focused on improving the print quality, reproducing colors more accurately and reducing printing artifacts. More recently, the tendency of controlling additional aspects of the print has been observed, including managing the optical surface characteristics, such as the shininess or glossiness, and creating physical texture[2] by piling up layers of ink into the third dimension.

In the current state of 3D printing systems, where applications range from creating prosthetics to parts replacement and fast prototyping, there is limited control of color and reflection properties. This is mainly due to the fact that most common 3D printers use a single or limited number of materials with which the 3D object is built, often with low resolution accuracy. These printing systems are primarily used for functional applications, where the surface appearance is of minor importance. On the other hand, printing applications with an important aesthetic component, such as jewelry, art or clothing, require a stronger focus on the resulting surface appearance.

Besides 3D printing, several applications of 2D printing systems would also require the ability to control the angular dependent reflection properties and translucency of the printed surface. The reproduction of material appearance can be seen as an application, where a print can be reproduced with perceptually similar appearance of texture, color and reflection properties to an original material. In aesthetic fields such as architecture and interior design, printing systems require accurate and extensive control of colors and textures combined with shiny, sparkling and translucent looks to create printed surfaces and panels for decoration and facades. For applications related to publicity and communications, such as packaging and signaling, assuring that the observer's attention is drawn to a particular area of a print can be achieved by locally varying surface appearances producing metallic, shiny, sparkling, translucent, sandy and matte appearances, which we refer to as special effects. Besides aesthetic purposes, proper management of gloss levels of print surfaces could play an important role in anti-counterfeit applications.[1,2]

Although recent advances in 3D printing technology have led to improvements in the print surface experience, the technology is still in a premature stage. This is mainly due to technological limitations as well as the lack of standardized surface reproduction workflows. Available printing systems strongly vary in the number of ink channels that are

▲ IS&T Member.

Received June 3, 2015; accepted for publication Aug. 13, 2015; published online Nov. 05, 2015. Associate Editor: Marius Pedersen.

1062-3701/2015/59(6)/060404/14/$25.00

[2] Although the term 'texture' is often used to refer to a repeated flat 2D pattern, in this article we refer to physical texture, as a tactile aspect of a surface. Such a texture can be rough or smooth, and depending on the dimensions of the texture, variations can be visible to the naked eye (e.g., macroscale texture) or invisible (e.g., microscale texture).

©2016 Society for Imaging Science and Technology
DOI: 10.2352/ISSN.2470-1173.2016.9.MMRMA-361

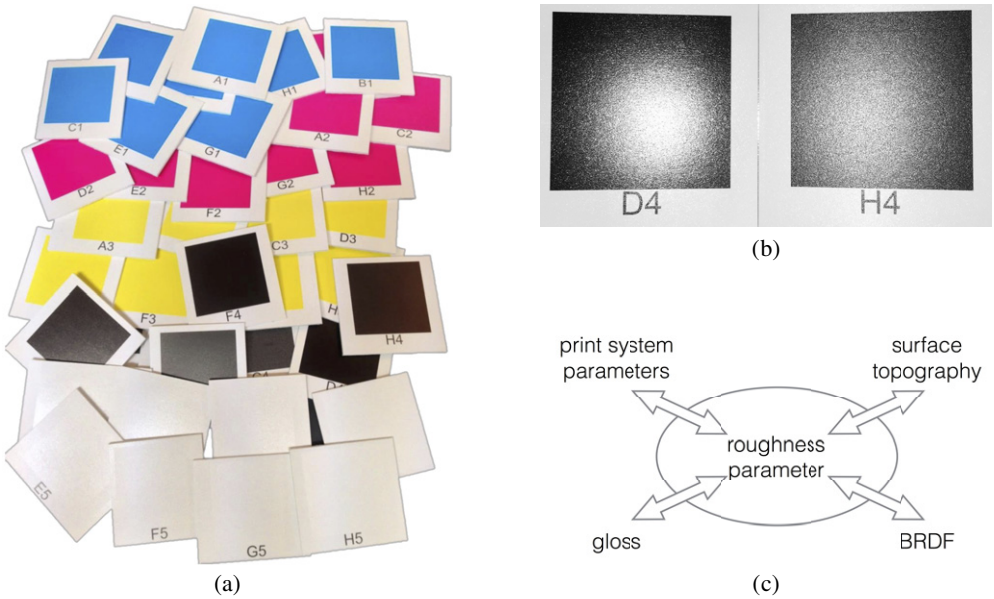

Figure 1. A set of patches (a) was printed utilizing different print parameters, resulting in variations of color and surface reflection properties, as seen for the reflection of a flash light on two of the samples (b). These print parameters affect both the geometric aspects (e.g., topography) and the optical characteristics (e.g., gloss, BRDF) of the surface. We investigate our hypothesis that variations in these geometric and optical aspects of our printed surfaces can be described by a single roughness parameter, as implied in (c). This knowledge is then used to manage the gloss level of printed surfaces by altering the surface topography on the micro-level basis to obtain the corresponding roughness level.

used, the resolution of the printing, their color palette and the size of smallest details that can be achieved. Due to the wide variation of materials that are used in newer printing systems, ranging from polylactic acid filaments to colored inks, metals and ceramics, the range of reproducible surface appearances varies across distinct technologies. Color management workflows are well established, but none of these workflows have been established for handling 3D surface and gloss properties. Although standards to handle 3D models, such as ISO[3] and ASTM,[4] have been developed for imaging, transferring and reproduction purposes, 3D workflows are still dysfunctional in many cases since there is no focus on perceptual appearance. Although the International Color Consortium (ICC) has shown recent progress with the creation of the iccMAX,[5] a workflow that handles fluorescence and additional ink channels, an additional color pipeline would be required to be able to manage both color and gloss simultaneously.

In addition to limitations of current printing systems for the creation of surface texture, the control of optical surface characteristics is considerably limited as well. When comparing the state of the art methods for the control of optical surface characteristics of prints, we can distinguish between two main approaches: either additional inks are added to an existing printing system to obtain a wider range of reflection properties (metallic ink, varnish, etc.) or the surface topography is modulated to affect the resulting reflection properties (often referred to as BRDF fabrication). The former approach imposes hardware challenges, as there are not very many printing systems supporting the addition of extra ink channels. Moreover, estimation of the extent and type of extra channels needed to reproduce a given set of surfaces would increase the complexity of this approach. The latter approach is difficult to obtain with currently available surface fabricating machines and 3D printing systems due to their limited ability to modulate surfaces at high spatial frequencies, which results in visible texture artifacts.

In this article we present our strategy to control the optical surface characteristics of a print, exclusively by modulating the roughness of the surface on a sub-millimeter scale, which is invisible to human observers. We achieve this by locally varying printing parameters such as multi-pass print strategies, ink deposition methods and curing methods, which affect the optical properties as well as the microscale surface topography. As an example, patches varying in color and reflection properties are shown in Figure 1.

Based on preliminary measurements of printed surfaces, we hypothesize that a single roughness parameter can be used to describe the variations of both optical and geometric surface characteristics of our printed patches, as indicated in Fig. 1(c). This idea is further investigated by relating measurements of geometric and optical aspects of the printed surfaces, as presented in the second half of this article. This single roughness parameter is then used in our work to estimate surface reflection properties such as BRDF and glossiness from the print surface geometry and vice versa. Furthermore, the surface roughness is used as a control parameter to manage the gloss of a print, by modulating the surface on a microscale level.

©2016 Society for Imaging Science and Technology
DOI: 10.2352/ISSN.2470-1173.2016.9.MMRMA-361

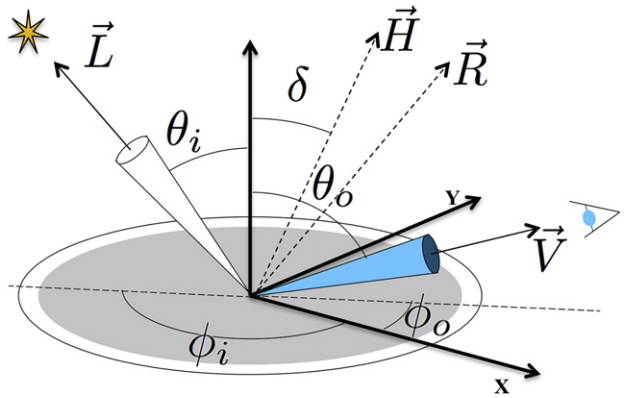

Figure 2. Coordinate system for BRDF, where the normal of the main surface is oriented in the Z direction. The direction of the incoming light is described by the vector $\vec{L}$ based on the zenith angle θ_i and the azimuthal angle ϕ_i. Similarly, the vector $\vec{V}$ represents the direction of observation defined by θ_o and ϕ_o. $\vec{H}$ is the half vector between $\vec{L}$ and $\vec{V}$, defined by angle δ.

RELATED STUDIES

Capturing and Modeling Surface Characteristics

The capturing and modeling of optical and physical surface characteristics is relevant for material surface rendering and reproduction. For printed surfaces we are mostly interested in the reflection properties describing the light–material interaction through BRDF functions. Here, the BRDF $\rho_{bd}(\theta_i, \phi_i, \theta_o, \phi_o)$ measures the ratio of outgoing radiance to incoming radiance defined in a 4D angular space, where the angles θ_i and ϕ_i describe the direction of the incoming light, and the angles θ_o and ϕ_o describe the viewing direction, as illustrated in Figure 2.

Various analytical models[6–10] have been proposed in the past to represent measurements of BRDFs. In general, an analytical model ρ is composed of a component ρ_d, describing the diffuse reflection (often assumed to be Lambertian), and a specular component $\rho_s K$, represented as follows:

$$\rho(\theta_i, \phi_i, \theta_o, \phi_o) = \rho_d + \rho_s K(\theta_i, \theta_o, \phi_o, \phi_i, k), \qquad (1)$$

where K is a function of the analytical model for specular reflection with model parameters k. In the simple form of the BRDF model from Eq. (1), only ideal diffuse and one single lobe of ideal specular reflection are assumed to exist, while no other directional components are considered. This common form has been shown to represent a wide range of different surface reflection measurements.

Research[10–13] has focused on the creation of error metric functions to quantify differences between two BRDFs. These functions vary both in the distance metric and in the weight applied to different components of the BRDF. Nevertheless, a perceptual error metric has not been developed yet. In fact, Ngan et al.[11] focused on fitting popular analytical models to measured BRDFs, using a standard error metric based on a Euclidian metric. The metric showed the ability to compare the fitting of different BRDF models. The difference between two BRDF functions ρ_a and ρ_b is defined as the root mean square average of the radiance difference for all measured points Ω:

$$E(\rho_a, \rho_b) = \sqrt{\frac{1}{\sum_\Omega} \sum_\Omega [\rho_a \cos(\theta_i) - \rho_b \cos(\theta_i)]^2}. \qquad (2)$$

The $\cos(\theta_i)$ term is introduced under the assumption that for illumination angles closer to the grazing angle, measured BRDFs and analytical models are less accurate and therefore less weight is applied to these angles. Several studies such as those of Lafortune et al.[10] and Fores et al.[12] have discussed the use of other error metrics and approaches for BRDF sampling as well;[13] however, it is mentioned that only a minor difference in the behavior is observed on low gloss anisotropic samples.

Gloss is an important aspect of material appearance and is usually measured using a gloss meter. Although gloss can be related to physical measurements and BRDF properties, it is often associated with perceptual appearance. Hunter[14] was the first to explore the multi-dimensionality of gloss, and defined six criteria for ranking surfaces based on their gloss levels: specular gloss, sheen, contrast gloss, absence of bloom, distinctness of image (DOI) and surface uniformity. Gloss meters are used to measure the amount of specular reflected light by determining the ratio of reflected light to the incident light for the opposite angle as defined by an ISO standard.[15] Leloup et al.[16] proved the relationship between gloss and BRDF measurements and showed the limitations of using a gloss meter for gloss measurements, where gloss is measured as a one-dimensional attribute and strong differences exist between several gloss meters.[17]

Besides the optical surface characteristics, physical characteristics are an important contribution to the appearance of the material surface. Roughness is one of the most frequent descriptors of physical properties and is commonly defined as the amount of physical texture. The perception of appearance of physical texture is strongly dependent on the scale of the roughness variations. Westin et al.[18] distinguished different scales of physical surface texture, such as the micro-, milli- and object scale. In the millimeter scale, texture variations are considered to be observable as physical texture, while finer scale (micro) texture variations are responsible for optical characteristics such as the BRDF. In this article we mainly focus on the roughness at the microscale, which is not directly visible by the human eye, but affects the reflection properties of the surface.

Geometric versus optical characteristics

The roughness of a surface geometry is used in most BRDF models as a parameter of the reflection properties of a surface, where "rougher" surfaces correspond to more diffuse surface reflections. Research in several fields has focused on the relationship between geometric surface characteristics such as surface roughness and optical properties such as gloss. Studies[19,20] for dental applications have focused on the relationship between gloss and roughness, showing the trend of decreasing gloss with increasing roughness. Xu et al.[21]

DOI: 10.2352/ISSN.2470-1173.2016.9.MMRMA-361

performed measurements of print surface roughness by using a stylus profilometer and an atomic-force microscope to determine correlations with gloss meter measurements. Beland et al.[22] performed similar experiments using an atomic-force microscope to measure the topography of samples locally and were able to relate these measurements to the local gloss levels of their samples. Furthermore, significant correlations between measurements of gloss and roughness of black prints have been shown by Juuti et al.[23] These studies have focused on relationships between geometric and optical surface characteristics for several materials, but gloss and color varying patches from digital printing systems have not yet been considered. In our work, we focus on this relationship, which could be used to better understand the appearance and artifacts of printed samples as well as to control the optical surface characteristics.

The relationship between the microscale surface topography and the resulting BRDF has been modeled by several authors who have simulated microscale scattering events. Some studies[9,24,25] have focused on the relationship between the microscale surface topography, as described by a microfacet distribution function, and the BRDF of a surface. These models have been verified by authors such as Baba et al.[26] and have been used for computer rendering of printed samples. Most of these models are mainly used for computer graphics, and only little research has focused on the application of these models to predict optical properties of material surfaces based on geometric properties.

The effect of roughness variations on surface colors of building stones was studied by Benavente et al.[27] Their research showed an increase of lightness and a reduction of chroma with increasing roughness, which can be explained by more scattering of specular reflection occurring on rough surfaces. Briones et al.[28] used chocolate samples with identical material properties but different roughness scales and measured their color, gloss and surface topography. Even though their experiments focused on a small selection of materials and gloss variations, relationships among gloss, texture and color were found in their work.

Surface reproduction

An upcoming area of research is related to surface appearance reproduction based on material surface descriptors (e.g., in terms of color, texture and BRDF). While color management of reproduced surfaces is well established and workflows for 3D texture information for printing applications are progressively improving,[15] the management of reflection functions, such as BRDF and gloss, is still at an early stage. Reproduction of the appearance of a given material using a printing system is a challenge due to the limited control of aspects such as surface texture and reflection properties.

Since standard printing systems use a small set of (typically four) ink channels to produce an intended color, there is minimal control of other reflection properties. However, in a study presented by Matusik et al.,[29] additional inks were added to a printing system with varying reflection properties to approximate an intended BRDF. Unfortunately, the method works only when additional inks are incorporated into the printing system and can result only in isotropic BRDFs.

Another example of research with the goal of printing spatially varying reflectance functions was presented by Malzbender et al.[30] The major advantage compared with the work by Matusik et al.[29] was that the reproduction was not limited to isotropic BRDFs. A lens-like paper was combined with precise dot placement to control the image appearance from different illumination and viewing directions. In this approach, a reflectance function is extracted from a target image for each pixel location. This reflectance function is reproduced by printing opaque ink on the reflective substrate, forming a specular highlight only at the point where no ink is applied. Regarding anti-counterfeit applications, Wang et al.[31] were able to control the angular dependent appearance of the print by orientating the anisotropic halftone screen locally, at the expense of not being able to produce isotropic reflection functions.

Another approach is to modulate the surface topography to influence the reflection properties locally. Through the use of a milling machine, Weyrich et al.[32] controlled the BRDF of a sample by changing the orientation of small facets on the surface corresponding to the intended BRDF. Similarly, Alexa and Matusik[33] showed that reflection functions of a surface could be managed by modulation of the surface height locally. Using a 3D printer, Rouiller et al.[34] created 3D objects of which the surface was modulated on the micro level to control its reflection properties. Moreover, Lan et al.[35] used a 3D printer to control the orientation of the microfacets on the print surface in combination with an ordinary color printer. While the control of reflection properties is achieved in these methods by modulating the surface texture, the systems are limited by the scale at which the surface is controlled and the color palette they can handle, and an additional system is required in most cases. This leads to visible texture artifacts and a dismissal of aesthetic aspects.

By obtaining an understanding of the relationship between physical and optical characteristics of printed samples, we propose a color and gloss management system where the gloss level of printouts is managed by determining the corresponding roughness levels on a microscale. In the following section we discuss our proposed workflow for gloss management by variation of print parameters. Hereafter, we present the measurements of both physical and optical surface characteristics of our printed samples and investigate the relationships between these measurements. Finally, we discuss the findings of work and draw conclusions.

GLOSS MANAGEMENT FOR PRINTING

We propose a workflow to manage gloss levels locally by modifying distinct print parameters. In contrast to the work described in the previous section, our strategy does not require additional inks or systems. The gloss levels of the print are managed through modulation of the print roughness at a micro-level scale, introducing texture

DOI: 10.2352/ISSN.2470-1173.2016.9.MMRMA-361

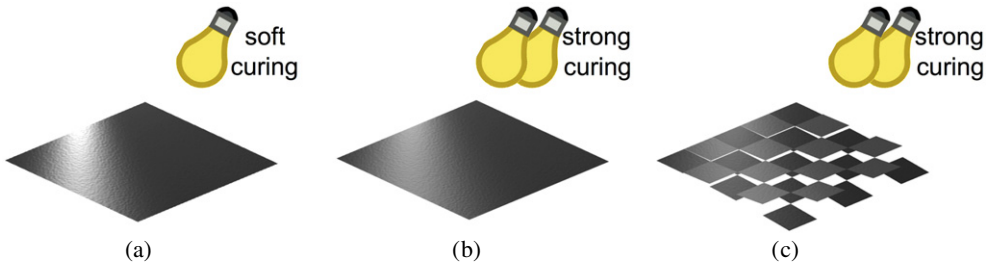

Figure 3. Schematic representations of three print modes. While depositing the same amount of ink, the gloss level can be altered from a glossy (a) to a matte appearance (c), by changing the UV-curing intensity (a versus b and c) or by using a multi-pass mode, where droplets on neighboring pixel locations are deposited in different layers, to produce an even more matte appearance (c).

artifacts invisible to the naked eye. The local changes of gloss are achieved by making use of the surface reflection properties resulting from different print parameter settings. The method builds upon our previous work where we have shown how the surface gloss level can be altered by influencing the ink drying/curing properties and multi-pass strategies.[36,37]

Depending on the printing technology, several parameters of the print system can influence the micro-surface roughness of the print. Although the settings of these parameters are usually overseen, or only considered as a trade-off between print quality and print speed, we propose to use them as a way to control the micro-surface characteristics and, in consequence, the reflection properties such as gloss. Therefore, we start by attempting to comprehend the effect of different print parameters on the micro-surface topography and reflection properties, to later construct a workflow where print parameters are selected based on an intended gloss level or BRDF properties.

Print parameters and surface characteristics

In a common print system, distinct settings can result in variations of surface reflection properties, even in cases where the same amount of ink is placed on the medium. For instance, multi-pass print strategies, where adjacent pixels are printed in different passes, are known to affect the surface roughness and thereby the BRDF properties.[38] The strategy that can be used to alter the reflection properties of the printout may vary from one system technology to another.

In Figure 3, a schematic representation of print parameter variations for a UV-curable printing system with several multi-pass print modes is presented. The diagram indicates how the gloss level can be affected by changing the UV-curing intensity or by using a multi-pass print mode. The more matte appearance of Fig. 3(c) is the result of printing the image through several passes.[36] Such a multi-pass print job is obtained by dividing the total amount of ink over a number of passes or layers, each containing a fraction of the total intended ink. The combination of passes results in a rougher surface with a more matte appearance compared with a single-pass strategy (Fig. 3(b)). On the contrary, the glossier patch of Fig. 3(a) is obtained by printing all intended ink in a single pass and by setting the ink curing parameters to a lower level to allow more time for the liquid ink to spread on the print surface before it is solidified. This creates a smoother surface[37] with a glossier appearance. Variations and combinations of these parameters (to which we refer as "print modes" in the rest of this article) are used to obtain a wider variety of surface appearances.

Gloss Management Workflow

In principle, many parameters of the print system cannot be altered on a pixel-by-pixel basis even when proprietary access is granted. Nevertheless, we can overcome this limitation by splitting the image into different print passes to manage gloss locally. In this way, each pass uses a set of parameters that is meant to achieve a given level of gloss. Such a workflow is presented in Figure 4, and indicates how a print is constructed with several passes. The following steps are involved in the process of gloss management.

(1) The intended color and gloss levels of the print are determined on a pixel-by-pixel basis.
(2) The color and gloss levels are mapped to the range of printable levels, and for each pixel, the print mode that results in the intended gloss level is determined.
(3) The image is divided into several passes, one per print mode, each pass containing only the image content that corresponds to the specific gloss level.
(4) The image is printed in different passes, where for each pass the print parameters are adjusted to the corresponding print mode settings.
(5) The resulting print presents intended gloss variations obtained by local adjustments of the print parameter settings.

Such a multi-pass print strategy is particularly easy to apply to 3D printing systems, where structures are already printed in various superimposed passes.

The most essential part of the workflow of Fig. 4 is determining the print mode that corresponds to the intended reflection properties (step 2 above). Relating the print modes to the physical processes that are involved during ink deposition and curing, for the estimation of gloss and texture characteristics, is out of the scope of this work. We focus on the resulting geometric surface characteristics of the print, in particular the surface roughness, which is expected to be a characteristic of a given print mode and

DOI: 10.2352/ISSN.2470-1173.2016.9.MMRMA-361

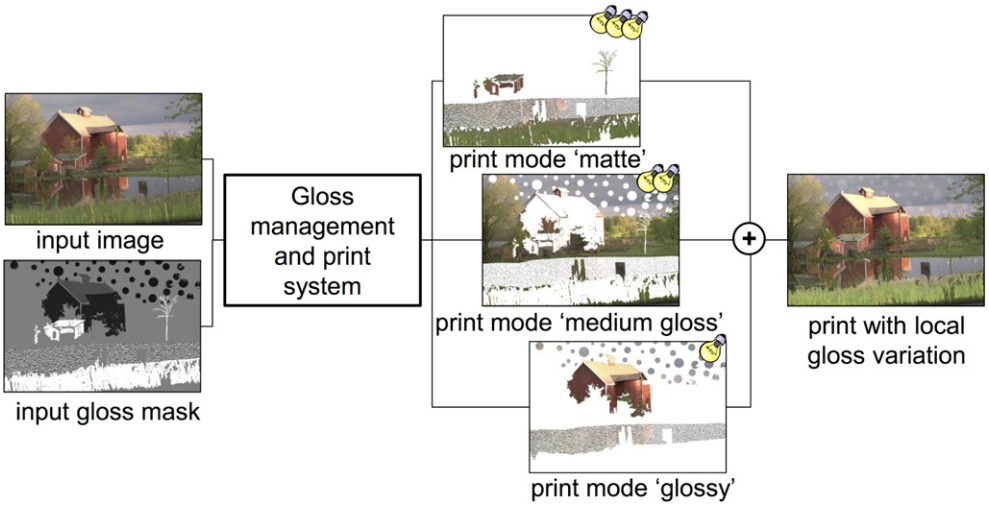

Figure 4. Workflow to achieve a print with local gloss variations. The input contains local color and gloss information. The content of each intended gloss level is printed with a corresponding print mode determined by the gloss management workflow. The outcome is a print that presents different levels of gloss.

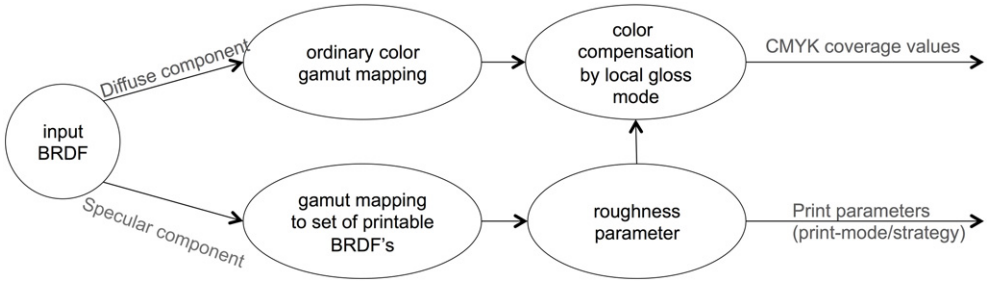

Figure 5. Workflow of gloss/BRDF management, where the ink coverage values and print parameters are determined based on an intended BRDF appearance. The print parameters are linked to a BRDF via the roughness characteristics of the resulting print surface.

can be related to optical reflection properties. Our hypothesis is that there exists a simple relation between the geometric and optical surface properties such as gloss, characterized by the roughness level of the surface topography. The roughness level is then used as a link between the intended reflection properties and the available print modes as follows (see Figure 5), describing step 2 (above) in more detail.

(1) The intended BRDF (or input of gloss and color information) is first split into a color (e.g., diffuse) component and a specular component. The color information is mapped to the color gamut of the print system, and the specular part is mapped to the space of reflection functions that are printable by the printing system.
(2) The ink coverage values are specified from the mapped color using a standard color management approach.
(3) The model that relates reflection properties with surface roughness levels is used to find the print parameter combination that provides the geometric surface characteristics corresponding to the mapped reflection function.
(4) In cases where the chosen print parameters are known to affect colors, a color compensation step is introduced.[39]

Implementation of Gloss Management Workflow

Our workflow, depicted in Fig. 4, was implemented using two prototype ink-jet printers: a wet-on-wet system and a wet-on-dry UV-curing-type system. Both systems allow the superimposition of several layers of ink on the same printing area as well as the manipulation of a number of parameters that affect the print surface roughness.

In the wet-on-wet printing system, where a gel ink is jetted onto the medium and crystallized (cured) by a heating system, gloss variations were created without requiring additional inks or systems. The time between the placement of each ink layer proved to be an important parameter to obtain the desired gloss level.[36] Using the time between printing different layers as a parameter, print modes were created for gloss variations of between 2 and 20 gloss units (for the 60° measurement angle).

Similarly, print modes were used on the wet-on-dry UV-curing printing system to modulate gloss levels locally. Each layer of ink is polymerized by UV light, allowing the next layer to be printed on a dry surface. Using this printing system, both multi-pass strategies and control parameters for the UV exposure mechanism were used to alter the surface roughness and reflection properties.[37] Through the variation

©2016 Society for Imaging Science and Technology
DOI: 10.2352/ISSN.2470-1173.2016.9.MMRMA-361

of these parameters, gloss levels were controlled to between 10 to 35 gloss units.

The proposed gloss management workflow has shown to be suitable for controlling gloss levels by varying parameters of the printing system. For the proper management of gloss and color, the workflow requires an understanding of the actual relationship between applied geometric surface characteristics and resulting optical properties. Therefore, we conducted an experiment in which the optical and geometric characteristics of printed patches were measured, as presented in the following sections.

MEASUREMENTS OF PRINT SURFACE

A set of patches was printed using different print modes, varying both surface color and microscale texture properties. The patches were printed using the wet-on-dry UV-curing ink-jet printing system, where multi-pass print strategies and variations of the UV light intensities were combined, giving a total of eight different print modes. Cyan, magenta, yellow, black and white patches were created using each of the print modes, resulting in 40 patches with five color variations for each of the eight print modes. Two underlayers of white ink were printed before the actual print to cancel out the effects of the roughness of the medium.

For each of the printed patches (presented in Fig. 1), several surface measurements resulted in four roughness parameters ($Ra, \sigma_{\mathrm{ADF}}, m_B, m_P$) based on topographic methods and seven parameters ($g_{20}, g_{60}, g_{85}, \alpha_{\mathrm{BP}}, \alpha_W, \alpha_{\mathrm{CT}}, \alpha_{\mathrm{AS}}$) based on optical methods. These parameters were chosen based on their popularity in the fields of material surface characterization and computer graphics. Although each of the parameters refers to the same property of the surface (i.e., the roughness), methods for their measurement and computation strongly differ. The exact calculation of these parameters is described in the remainder of the article, as well as an investigation of the relationships between the 11 roughness parameters.

Surface Geometry

A Dektak 150 stylus profilometer was used to retrieve one-dimensional surface profiles for each of the patches, from which roughness parameters were calculated. Roughness profiles of the print surfaces were obtained from the measured surface profiles, according to the ASME standard for measurements of surface texture.[40] Since the typical thickness of one single ink layer in our setup is around 1.7 µm, roughness variations of the printout can be expected in the same order of magnitude. Therefore, measurements were conducted for a traversing length of 6 cm per printed patch with a 1 µm horizontal resolution and 1.85 nm vertical resolution using a stylus tip with a radius of 5 µm. Furthermore, the roughness profile $Z(x)$ was extracted from the measured profile using a band-pass filter with a long wavelength cut-off frequency λ_c of 1 mm and a short wavelength cut-off frequency λ_s of 8 µm. From the obtained roughness profile $Z(x)$ (or Z_i for discrete measurements with N patches), roughness values were calculated. First, the widely used statistical roughness average Ra (µm) was determined by

$$Ra = \frac{1}{L}\int_0^L |Z(x) - \bar{Z}|dx = \frac{1}{N}\sum_{i=1}^{N} |Z_i - \bar{Z}|. \tag{3}$$

A second common roughness parameter σ_{ADF} (µm) was extracted from the amplitude density function (ADF), a histogram of the surface height. Here, σ_{ADF} is calculated as the standard deviation of the roughness profile Z_i around the mean surface $\bar{Z}$:

$$\sigma_{\mathrm{ADF}} = \sqrt{\frac{1}{N}\sum_{i=1}^{N}(Z_i - \bar{Z})^2}. \tag{4}$$

In contrast to the roughness parameters from Eqs. (3) and (4), which are measures of the height variation of the roughness profile, we expected a better correlation with optical measurements when roughness parameters were extracted from local surface slope distribution functions. After all, popular light reflection models are based on slope distribution functions (i.e., microfacet distribution functions). Here, the measured surface is assumed to be composed of many small facets, each characterized by the angle Θ_i between the normal vector of the microfacet i and the normal vector of the mean surface. Based on the obtained surface profile Z_i with measurement resolution r (i.e., horizontal distance between measurements Z_i and Z_{i+1}), we determined Θ_i for each microfacet i connecting Z_i and Z_{i+1} by

$$\Theta_i = \tan^{-1}\left(\frac{Z_{i+1} - Z_i}{r}\right). \tag{5}$$

The microfacet distribution $H(\theta_m)$ is obtained by counting the occurrence of local gradients Θ_i of the surface profile in each angular direction θ_m (from $-15°$ to $15°$).

Two popular analytical microfacet distribution functions are the Phong and Beckmann functions, both based on a single roughness parameter. For a particular roughness level m_P, the Phong distribution function is described by

$$D_{\mathrm{Phong}}(\theta_m, m_p) = \frac{m_p + 2}{2\pi}\cos(\theta_m)^{m_p}. \tag{6}$$

Similarly, the Beckmann distribution function, based on the roughness parameter m_B, is described by

$$D_{\mathrm{Beckmann}}(\theta_m, m_B) = \frac{1}{\pi m_B^2 \cos(\theta_m)^4} e^{\frac{\cos(\theta_m)^2 - 1}{m_B^2 \cos(\theta_m)^2}}. \tag{7}$$

Each of the (dimensionless) parameters m_P and m_B from Eqs. (6) and (7), respectively, was determined by fitting the corresponding microfacet models to the measured distribution functions $H(\theta_m)$ for each patch, minimizing the distance between the two distributions for the Phong model:

$$\arg\min_{m_p} \int_{\theta_m=-15}^{15} \sqrt{(D_{\mathrm{Phong}}(\theta_m, m_p) - H(\theta_m))^2}, \tag{8}$$

©2016 Society for Imaging Science and Technology
DOI: 10.2352/ISSN.2470-1173.2016.9.MMRMA-361

and the Beckmann model:

$$\arg\min_{m_B} \int_{\theta_m=-15}^{15} \sqrt{(D_{\text{Beckmann}}(\theta_m, m_B) - H(\theta_m))^2}. \quad (9)$$

From the fitting of these analytical distribution functions, the roughness parameters m_P and m_B were determined based on the surface geometry measurements for each of the printed patches.

Gloss

As was concluded in our previous experiments, the BRDF functions resulting from different print modes show similar characteristics, differing only in the width and strength of the specular lobe. As a consequence, these differences can be well distinguishable with a simple measurement system such as a gloss meter. The gloss levels of all patches were measured by determining the amount of specular reflected light at angles of 20°, 60° and 85° using an MG628-F2 multi-angle gloss meter. The gloss value is measured in gloss units (GU), where a GU is defined in such a way that a glossy material with a refractive index of 1.567 has a value of 100 GU for any illumination angle, according to the ISO standard for gloss measurements.[3]

BRDF

In reality, the BRDF of a surface is wavelength dependent and describes the amount of reflected light in a particular direction, which requires complex and time consuming measurements. However, for a non-complex BRDF such as that of printed patches, the reflection properties can be approximated by an isotropic BRDF with one single lobe of specular reflection and a reduced sampling of the full BRDF. Using a commercially available instrument by Light Tec called MiniDiff, scattering measurements of the printed patches were obtained for incoming illumination angles θ_i of 0°, 20°, 40° and 60°, where the patch was illuminated at a single wavelength of 622 nm. The reflected light was measured in the hemisphere described by observation angles θ_o from 0° to 75° and ϕ_o from 0° to 360°, both with an angular resolution of one degree. An analytical description of the full BRDF was recovered by fitting the measurements to popular BRDF models.

We used six BRDF models to approximate the BRDF of each printed patch based on the obtained scattering measurements. These models included two empirical Phong and Blinn–Phong[6] models, which are mainly used for computer graphics applications, two theoretical models, Cook–Torrance[8] and Ashikhmin–Shirley,[9] which are based on the physical theories of surface reflection, and two experimental Ward[7] and Lafortune[10] models, which are constructed by analyzing BRDF measurements of real world surfaces. We consider the general form of the BRDF according to Eq. (1), where the diffuse component is assumed to be Lambertian, and the specular component is described by the analytical model K with model parameters k. The model parameters k include, depending on the model used, one or more roughness parameters α and material parameters such as the Fresnel coefficient F_0. For instance, we fit a particular BRDF measurement ρ_{meas} by the Cook–Torrence model K_{CT} with roughness parameter α_{CT} and additional parameters k, such that a fitted model ρ_{fit} is described by

$$\rho_{\text{fit}}(\theta_i, \phi_i, \theta_o, \phi_o) = \rho_d + \rho_s K_{\text{CT}}(\theta_i, \phi_i, \theta_o, \phi_o, \alpha_{\text{CT}}, k). \quad (10)$$

Since every set of eight patches contains an equal amount of the same colorant only differences were assumed to be present in micro-surface topography. Following Eq. (10), we can expect that, for the whole set of patches with identical inks, the diffuse and specular reflection coefficients (ρ_d and ρ_s) are identical, as well as the values of intrinsic material parameters k, such as the Fresnel coefficient (F_0). Thus, we modeled variations between different patches exclusively by the roughness (α), presented as one single parameter in each of the analytical BRDF models used. The roughness parameters α_n were determined for each set of BRDF measurements $\rho_{\text{meas},n}$ of N patches with identical colorants such that the sum of differences between the measured BRDF and the predicted BRDF using the analytical models was minimal:

$$\arg\min_{\rho_d, \rho_s, \alpha_1 \ldots \alpha_N, k} \sum_{k=1}^{N} E(\rho_{\text{meas}}(n), \rho_{\text{fit}}(\rho_d, \rho_s, \alpha_n, k)). \quad (11)$$

The distance E between the measured and approximated BRDF was calculated according to Eq. (2).

RESULTS FROM COMPARATIVE ANALYSIS OF SURFACE MEASUREMENTS

Roughness parameters were obtained from optical and geometric surface measurements of printed patches with variations in color and gloss levels as described in the previous section. Our hypothesis is that we can describe the relationship between optical and geometric surface characteristics by a first- or second-order polynomial function, as has been shown for a handful of surfaces in previous research.[19–28]

Roughness Profile

Roughness parameters were extracted from surface profile measurements of the print using a stylus profilometer. Measurements made by this device are known to contain minor instabilities, which occur due to external vibrations around the scanning stylus. To evaluate the accuracy of the profilometer we therefore compared the obtained surface profiles with 2D surface measurements using a digital holographic microscope (Lyncée Tec). The images of Figure 6 present two of the obtained height maps, presenting a smooth glossy patch and a rough matte patch. These topography measurements clearly indicate that the matte patch is rougher with higher spatial frequency variations than the glossy patch. When comparing the measurements using the stylus profilometer and the 2D holographic microscope,

©2016 Society for Imaging Science and Technology
DOI: 10.2352/ISSN.2470-1173.2016.9.MMRMA-361

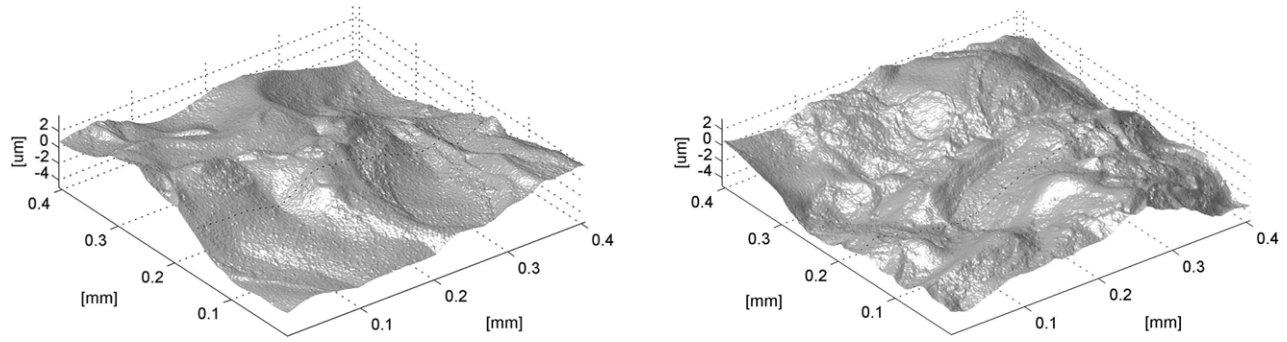

Figure 6. Surface topography measurements for a glossy patch (a) and a matte patch (b). Although the low spatial frequency height variations are very similar, high spatial frequency height variations are more visible in the measurement of the matte patch.

Table I. Roughness values and standard deviations of white patches for four different print modes. For each patch, the roughness values Ra, σ_{ADF} and m_B result from surface topography measurements, while the g_{60}, α_{BP} and α_{CT} result from optical measurements. Note that the values of Ra, σ_{ADF}, m_B and α_{CT} increase with the roughness of the print surface, while the values of g_{60} and α_{BP} decrease with the print surface roughness. Correlations between the different roughness parameters were investigated to examine the relationship between geometric and optical roughness parameters of prints.

	Print patch			
Parameter	White mode 1	White mode 3	White mode 5	White mode 7
Ra (μm)	1.78±0.05	1.71±0.09	2.48±0.06	2.74±0.07
σ_{ADF} (μm)	0.21±0.02	0.24±0.02	0.36±0.04	0.41±0.02
m_P	580±60	380±50	210±30	130±20
m_B	0.058±0.004	0.073±0.005	0.099±0.007	0.12 ±0.01
g_{60} (GU)	32.5±2.4	27.6±1.7	18.3±0.5	12.8±0.1
α_{BP}	372	340	195	104
α_{CT}	0.068	0.080	0.101	0.150

very similar dimensions of surface texture variations and roughness parameters were found. This indicates that for our application, the use of the stylus profilometer is sufficient for the characterization of our surfaces, despite providing only 1D surface profile measurements.

Roughness parameters Ra and σ_{ADF} were calculated in accordance with Eqs. (3) and (4) from the roughness profiles measured with the stylus profilometer. The statistical roughness average Ra ranged from 1.4 to 3 μm between the prints, as expected, given the fact that the printed surface consisted of several layers of ink with a typical thickness of around 1.7 μm. The first two rows of Table I present the measured roughness values for four white patches. They were printed with print modes 1, 3, 5 and 7, here sorted on decreasing gloss level. Even though noisy measurements resulted in high standard deviations, we were able to confirm that for an increment of roughness there exists a reduction of gloss.

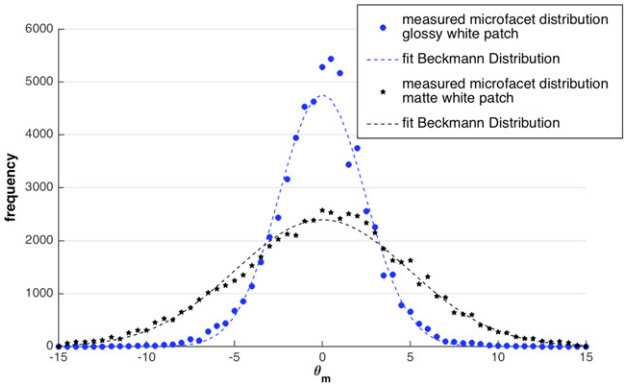

Figure 7. Microfacet distributions for a glossy and a matte patch extracted from the surface topography measurements. Beckmann distribution functions are fitted through these measurements to obtain roughness parameters for each of the patches.

Microfacet Distribution

Microfacet distribution functions were obtained from the roughness profiles for each of the 40 patches. The resulting distribution functions for a glossy and a matte patch are shown in Figure 7 together with the fitted Beckmann distribution curves from Eq. (6). A broader distribution indicates a rougher surface, which in turn corresponds to a matte patch. Only minor differences were observed between the resulting fitted curves using either the Phong or the Beckmann distribution function, which is a common observation for narrow shaped distribution functions, as mentioned by Kelemen and Szirmay-Kalos.[25] For the rest of the patches, we observed similar results to those of Fig. 7, where the Beckmann and Phong distribution functions closely represented the measured distributions. Based on the fitted Beckmann and Phong distribution functions, the roughness parameters m_B and m_P were obtained following Eqs. (8) and (9) for each patch (a subset is presented in Table I). Note that the roughness parameter m_B of the Beckmann function increases with the surface roughness while the roughness parameter m_P of the Phong function is smaller for rougher surfaces.

©2016 Society for Imaging Science and Technology
DOI: 10.2352/ISSN.2470-1173.2016.9.MMRMA-361

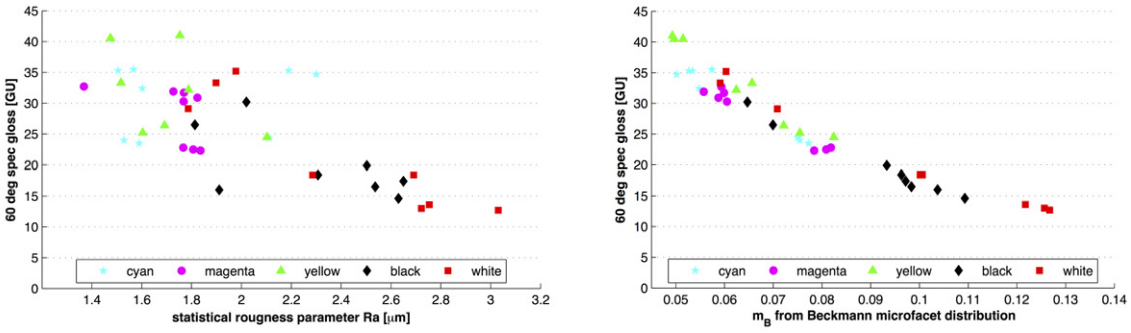

Figure 8. (a) Gloss level (obtained using a gloss meter) versus roughness parameter *Ra* (from stylus profilometer) for 40 printed patches ($r = 0.74$). (b) Relationship between surface gloss and roughness parameter m_B from Beckmann fit through microfacet distribution for 40 printed patches ($r = 0.96$). Note that even though the roughness values *Ra* and m_B are calculated from the same roughness profiles, m_B leads to better correlation with measured gloss levels.

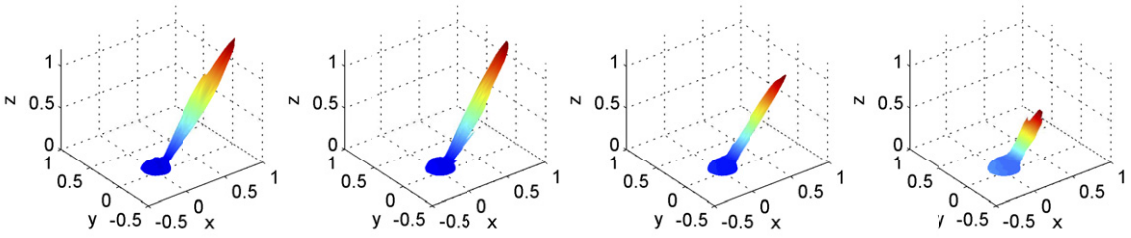

Figure 9. Surface scattering measurements extracted from magenta patches using four different print modes, ranging from a glossy (a) to a more matte reflectance (d). The surface is illuminated under an angle of 40° with a single wavelength illumination of 622 nm.

Gloss

Specular gloss values of between 12 and 41 GU were measured for the 60° measurement angle of the MG628-F2 multi-angle gloss meter. The black and white patches spanned a wider range of gloss values compared with the cyan, magenta and yellow patches, which is a result of the specific ink properties. The gloss values of the four patches indicated in Table I indicate the inversely proportional relationship with the surface roughness.

In Figure 8 this same relationship between measured gloss and roughness levels is found. From the graph of Fig. 8(a) we can see that the correlation between the statistical roughness average *Ra* (resulting from geometric surface measurements) and the measured gloss levels is fairly low; only a general trend is visible. However, when the gloss level measurements are related to the roughness parameters from the microfacet distribution (based on the same geometric surface measurements), a higher correlation is observed, as can be clearly seen in Fig. 8(b). This finding suggests that a roughness level extracted from the microfacet distribution represents the surface texture more accurately than the roughness parameter that is calculated as the RMS value of height deviations from the mean surface.

Light Scattering Measurements and BRDF Modeling

The roughness parameters of the analytical reflection models were found by fitting the model parameters to the BRDF measurements of the printed surfaces. BRDF measurements for an illumination angle θ_i of 40° are shown in Figure 9 for a selection of patches printed with magenta ink. A considerable decrease of the strength and a broader shape of the specular lobe are visible when we move from glossy patches toward more matte ones. Furthermore, the patches present an isotropic behavior, showing a Lambertian diffuse reflection with one single lobe of specular reflection.

The parameters of the analytical BRDF models were determined from the best fit to the measured BRDF data following Eq. (11). In Figure 10, a slice of the measured BRDFs is shown together with the fits of each of the analytical models. The measured reflection functions for all four illumination angles are shown, as well as the approximations by each of the analytical models. The fact that the models better approximate the measurements for smaller angles of illumination θ_i is due to the weight term $\cos(\theta_i)$ from Eq. (2). The more complex models, such as Ward and Ashikhmin–Shirley, were shown to better estimate the measured data. Furthermore, the theoretical Cook–Torrance and Ashikhmin–Shirley models were shown to perform well for glossy patches, while the empirical models provided better results for matte patches. The roughness parameters α_{BP} and α_{CT} corresponding to the fitted Blinn–Phong and Cook–Torrance functions are presented in the bottom rows of Table I. Note that α_{BP} decreases with the surface roughness while α_{CT} increases proportionally with the roughness of the surface.

©2016 Society for Imaging Science and Technology
DOI: 10.2352/ISSN.2470-1173.2016.9.MMRMA-361

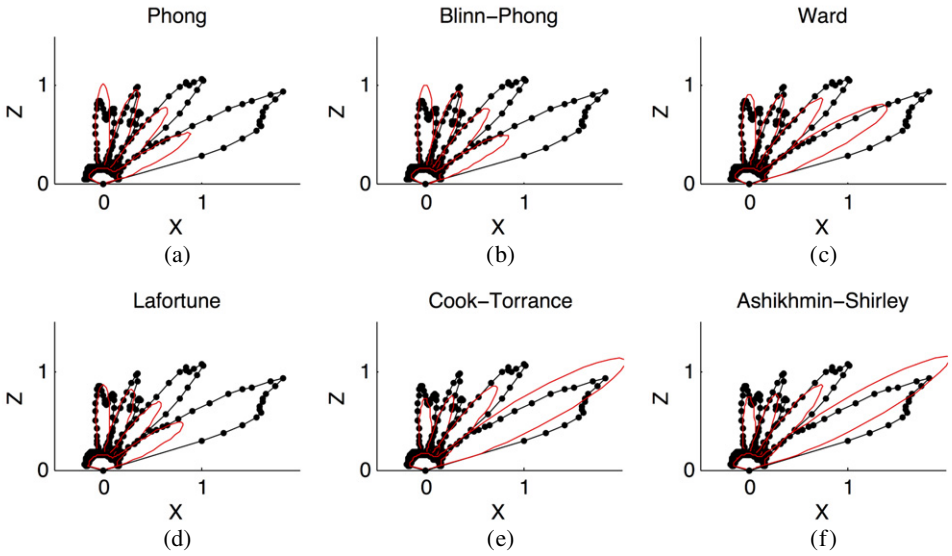

Figure 10. Polar plots of the light reflection in the incidence plane for four different angles of incoming light, along with the corresponding fits of the analytical model, for a white patch. The error metric from Eq. (2) was used to fit each of the analytical models to the measurements.

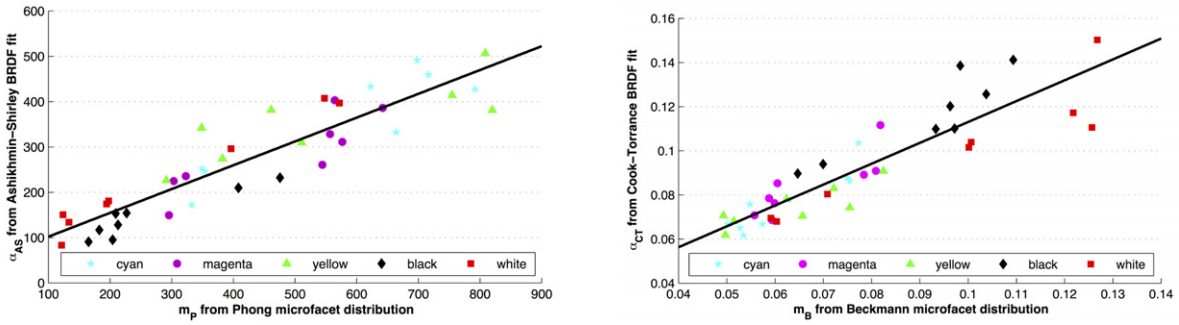

Figure 11. (a) Roughness parameter from the Ashikhmin–Shirley BRDF model versus roughness parameter from the Phong distribution curve through microfacet distribution ($r = 0.94$). (b) Roughness parameter from the Cook–Torrance BRDF model versus roughness parameter from the Beckmann distribution curve through microfacet distribution ($r = 0.90$).

Relating optical and geometric measurements of the print surface

Relationships between geometric and optical surface measurements were investigated for the purpose of understanding the influence of roughness on the optical properties such as BRDF and gloss. Since the printed patches present only minor variations in roughness and gloss, we assume that the relationship between surface roughness and optical properties such as gloss and BRDF can be approximated by a first-degree polynomial. To verify this assumption, we calculated the Pearson correlation coefficient between roughness values from surface texture measurements and optical measurements over all 40 printed patches combined, as indicated in Fig. 8.

Figure 11(a) presents the correlation between the roughness values α_{AS} as determined from the Ashikhmin–Shirley BRDF and m_P from the Phong microfacet distribution. The former is based on light scattering measurements and the latter is based on the measured roughness profile. Even though there exist only small variations in the patches and instabilities in both measurement devices, the method shows a fairly good correlation ($r = 0.91$). Similarly, Fig. 11(b) presents the relationship between the roughness values m_B and α_{CT}, with a similar correlation value ($r = 0.9$), indicating that surface roughness measurements estimate surface reflection functions quite well.

The Pearson correlation coefficient was determined for various combinations of optical and geometric roughness measurements assuming a first-order relationship, similar to the graphs in Figs. 8 and 11. All of the correlation coefficients are shown in Table II, from which it can be concluded that better estimates of optical characteristics can be made from roughness parameters from microfacet models (rows 3 and 4) than from surface height variations directly (rows 1 and 2). In addition, it is observed that roughness parameters better estimate the gloss levels than BRDF model parameters. Moreover, no significant difference is observed in using any of the analytical BRDF models tested in this study.

DOI: 10.2352/ISSN.2470-1173.2016.9.MMRMA-361

Table II. Absolute Pearson correlation coefficients between geometric characteristics (surface roughness parameters) and optical characteristics (average gloss values and BRDF roughness parameters).

Geometric	Optical						
	Gloss meter measurement			Roughness parameter BRDF model			
	20°	60°	85°	Blinn–Phong	Ward	Cook–Torrance	Ashikhmin–Shirley
	g_{20}	g_{60}	g_{85}	α_{BP}	α_{W}	α_{CT}	α_{AS}
Roughness average Ra	0.64	0.74	0.74	0.62	0.69	0.69	0.63
RMS amplitude density function σ_{ADF}	0.68	0.80	0.82	0.68	0.74	0.73	0.70
Beckmann parameter microfacet distribution m_B	0.87	0.96	0.96	0.88	0.91	0.90	0.88
Phong parameter microfacet distribution m_P	0.93	0.97	0.97	0.94	0.86	0.85	0.92

DISCUSSION

We investigated the relationship between micro-surface characteristics and optical measurements such as gloss and BRDF. The influence of the roughness of the medium on the reflection properties of the surface was discarded by depositing a few layers of white ink before the test patches were printed, assuming that the overall roughness would be mainly due to the topography of the outermost layers of ink. However, It is important to mention that the ink–medium interaction plays a relevant role for thinner layers of ink where the roughness of the medium can influence the gloss level of the surface.[21]

In this article, we have proposed a gloss management strategy where the microscale roughness of a print is controlled to generate an intended gloss level. We have shown that different surface roughness levels can be obtained by varying the print parameters. For this strategy to be applicable to commercial printers, several printing parameters need to be available for manipulation. In our experiments, we have shown its applicability on two different printing systems, where a set of print parameters was adjusted. Common (digital) printing systems, and in particular 3D printing systems, have the potential to be used in the same way, where parameters such as the single-pass or multi-pass print modes can be selected, so as to influence the surface roughness and thereby gloss levels. Nevertheless, a full implementation of this solution requires full control of the printing system and a specific system characterization step. Furthermore, depending on the system, more or fewer parameters can be altered, resulting in a corresponding wider or narrower range of printed gloss levels.

We restrict ourselves to the control of directly measurable aspects of the print surface, such as the physical surface roughness parameters, BRDF functions and gloss levels. However, it is important to mention relevant studies on the perceptual appearance of texture, gloss and BRDF models.[41–43] Obein et al.[44] and Leloup et al.[45] have focused on finding the relationship between gloss and BRDF measurements and the perceptual scaling of glossy samples by conducting psychophysical experiments using real-world samples. Through the use of printed samples including patches with different colors, Samadzadegan et al.[46] conducted similar experiments to find the link between perceived gloss differences and gloss measurements for a particular set of prints. Although in the initial stage, the construction of perceptual spaces for BRDF models and gloss is an ongoing field of research. Wills et al.[47] focused on constructing a Euclidian space where the distance between a pair of gloss samples matches the perceived difference of gloss by human observers. Perceptual spaces for BRDF models and gloss[12,48,49] have been designed to calculate the best visual match between an original and a reproduced BRDF. These perceptual spaces would be in particular interest to map intended surface representations to the space of reproducible reflectance functions, as shown in Fig. 5.

With respect to the investigated analytical BRDF models, the Ward model results in the best approximation of our BRDF measurements. On the other hand, for the surface characteristic measurements, we see that a simple model such as the Blinn–Phong model leads to higher correlations (Table II) with our data. In contrast to previous research, our results do not present the expected behavior of physical and more complex models to better fit BRDF measurements. As a matter of fact, the empirical Ward model outperforms the other investigated analytical models. Limitations and inaccuracies of the measurement systems as well as the more complex nature of the reflection properties of the printed patches could explain the poor representation of the BRDF measurements by physical and intricate BRDF models. However, the shape of the acquired BRDFs did not suggest the need for more complex analytical models that would include components such as directional diffuse[50] or multi-lobe specular reflections. The error metric from Eq. (2) can be changed for a more perceptual relevant metric, which could lead to more discrepancy between the performance of several analytical models, as proposed by Fores et al.[12] The uneven number of measurement points of the BRDF in the non-specular part resulted in a bias of the overall performance of one model over another. For example, the BRDFs of black and cyan patches were better estimated by each of the analytical models compared with the estimates made for the other colorants, which is due to the smaller diffuse component of these patches for the illumination

DOI: 10.2352/ISSN.2470-1173.2016.9.MMRMA-361

(622 nm) used in the setup. In future work, more accurate measurements of the BRDF could lead to better modeling of the surface reflection properties, which we expect to result in greater differences between the investigated BRDF models.

Even though previous research has mainly focused on the use of simple roughness parameters to correlate with gloss measurements, we observed better correlations with gloss measurements when the roughness was determined from the microfacet distributions. This can be explained by the fact that the inaccuracies introduced by sudden bumps or shocks in the stylus profilometer affect the overall measured profile, whereas the profile slope distribution is altered only to a small extent. Based on the extracted microfacet distribution, we observed better fits of the Phong and Beckmann distribution functions for glossier patches compared with more matte patches. Other microfacet distribution functions such as that discussed by Bagher et al.[51] and the GGX distribution function[52] may be investigated in future measurements.

Correlation coefficients between the geometrical and optical roughness parameters were calculated to determine the degree of the linear dependence between the parameters. This assumption might not be valid for a general case, where higher-order relationships have been found in previous studies.[27,28] Moreover, roughness parameters such as m_p and m_B have a completely different relationship to the actual surface roughness. We believe that the fact that the measured parameters could be fairly well related can be explained by the relatively small range of gloss and roughness levels between the printed patches, which could therefore be approximated by a linear relationship.

One topic that has not been addressed in this article is the effect of the surface roughness on the color of the printed patch, which is important to consider for accurate printed colors. In the study conducted by Farnand et al.[53] regarding the effect of gloss on color measurements, it was found that for low gloss and rough materials, scattered specular reflection desaturates the measured color. This effect was also visible in the color measurements of our printed patches, where noticeable color differences (up to $16\Delta E_{ab}$) were found for similar patches with different micro-surface texture characteristics. To accurately manage the surface color, the system would require a color management stage based on a set of characterization patches larger than the 40 patches measured so far, including ones with different ink coverage values and combinations of several inks. For that propose, we have proposed a color and gloss management workflow, which we have previously published.[39] Thereby, as shown in the gloss management workflow of Fig. 5, we introduce an extra step in the color management, where ink coverage levels are adapted to the print mode that is applied locally. In the proposed strategy, a separate color transformation is introduced for each print mode, each requiring characterization through the measurements of a set of printed patches. This implementation has been shown to considerably reduce the color differences between printed areas of different surface roughness.

CONCLUSIONS

A workflow for the management of color and gloss levels of printed patches is proposed, where the proper combination of colorants and print system parameters is determined based on the intended optical characteristics. Texture variations smaller than seen in the state of the art are introduced (with a single printing system) as a means to influence the reflection properties of the print surface. By controlling the optical characteristics through surface modulations at the microscale level, texture variations are not visible to the human eye and only the affected BRDF is observed.

Several parameters of printing systems, such as ink deposition and drying parameters, influence the surface microstructure, thereby affecting the optical properties such as the BRDF and gloss level. We present a gloss management workflow in which variation of the print parameters is used to control the optical properties. To investigate the influence of print modes on optical and geometric surface characteristics, we created a series of printed patches with a variety of colorants and print system parameters, from which attributes such as gloss levels, BRDF and surface topography were measured.

Based on our hypothesis that a linear relationship exists between the optical and geometric properties of printed surfaces, several surface characteristics were measured and correlations between the measurements were determined. Optical measurements, which included BRDF measurements, showed that out of several analytical BRDF models the Ward BRDF model best approximates the measured BRDF, presenting the smallest error. In addition to optical surface characteristics, roughness profiles were obtained from profilometer measurements, resulting in a microfacet distribution function corresponding to each patch. Based on these measurements, high Pearson correlation coefficients were found between roughness measurements and gloss levels as well as BRDF model parameters. These results indicate the suitability of using microscale roughness variations for the control of optical print characteristics, as the relationship between these attributes can be adequately predicted.

Findings from this work will result in a better understanding of the relationship between physical and optical properties of printed patches. Furthermore, the proposed color and gloss management process should be useful for applications ranging from material reproduction to security printings as well as rendering and soft proofing of printed patches.

ACKNOWLEDGMENTS

This work was supported by the Marie Curie Initial Training Networks (ITN) CP7.0 N-290154 funding. Furthermore, the authors would like to thank Frans Blom for his help with obtaining surface measurements using the stylus profilometer and the company Lyncée Tec for providing them with topography measurements of their prints.

DOI: 10.2352/ISSN.2470-1173.2016.9.MMRMA-361

REFERENCES

[1] C. H. Liu, S. G. Wang, and B. Xu, "Authenticate digital prints with glossmark images," *Proc. IS&t's NIP20: Int'l. Conf. on Digital Printing Technologies* (IS&T, Springfield, VA, 2004), pp. 312–316.

[2] A. Hodgson, "The use of gloss effects from inkjet printing for brand identification, personalization, and security," *Proc. IS&T's DPP2005: Int'l. Conf. on Digital Production Printing and Industrial Applications* (Springfield, VA, IS&T, 2005), pp. 108–109.

[3] ISO 14739-1:2014 Document management: 3D use of Product Representation Compact (PRC) format (ISO, Geneva), www.iso.org.

[4] ASTM E2807-2011, Standard Specification for 3D Imaging Data Exchange (ASTM International, West Conshohocken), www.astm.org.

[5] M. Derhak, P. Green, and T. Lianza, "Introducing iccMAX: new frontiers in color management," Proc. SPIE **9395**, 1–7 (2015).

[6] B. T. Phong, "Illumination for computer generated pictures," ACM Commun. **18**, no. 6, 311–317 (1975).

[7] G. J. Ward, "Measuring and modeling anisotropic reflection," ACM Comput. Graph. **26**, 265–272 (1992).

[8] R. L. Cook and K. E. Torrance, "A reflectance model for computer graphics," ACM Comput. Graph. **15**, 307–316 (1981).

[9] M. Ashikhmin, S. Premože, and P. Shirley, "A microfacet-based BRDF generator," *Proc. 27th Annual Conf. on Computer Graphics and Interactive Techniques*, (2000), pp. 65–74.

[10] E. P. F. Lafortune, S. C. Foo, K. E. Torrance, and D. P. Greenberg, "Non-linear approximation of reflectance functions," *Proc. 24th Annual Conf. on Computer Graphics and Interactive Techniques* (1997), pp. 117–126.

[11] A. Ngan, F. Durand, and W. Matusik, "Experimental analysis of BRDF models," *Proc. 16th Eurographics Conf. on Rendering Techniques* (2005), pp. 117–126.

[12] A. Fores, J. Ferwerda, and J. Gu, "Toward a perceptually based metric for BRDF modeling," *Proc. IS&T/SID CIC20: Twentieth Color and Imaging Conf.* (IS&T, Springfield, VA, 2012), pp. 142–148.

[13] G. Obein, J. Audenaert, G. Ged, and F. B. Leloup, "Metrological issues related to BRDF measurements around the specular direction in the particular case of glossy surfaces," Proc. SPIE **9398** (2015).

[14] R. S. Hunter, "Methods of determining gloss," J. Res. Natl Bur. Stand. **18**, 19–39 (1937).

[15] ISO 2813-2014 S. Paints and varnishes—determination of gloss value at 20 degrees, 60 degrees and 85 degrees ISO (ISO, Geneva), www.iso.org.

[16] F. Leloup, P. Hanselaer, J. Versluys, and S. Forment, "BRDF and gloss measurements," *Proc. CIE Expert Symposium on Visual Appearance* (2007), pp. 28–33.

[17] L. Ye, S. Banach, and J. Arney, "Interpretation of gloss meter measurements," J. Imaging Sci. Technol. **50**, 567 (2006).

[18] S. H. Westin, J. R. Arvo, and K. E. Torrance, "Predicting reflectance functions from complex surfaces," *Proc. 19th Annual Conf. on Computer Graphics and Interactive Techniques*, (1992), pp. 255–264.

[19] A. Fernández-Oliveras, M. F. M. Costa, A. Yebra, M. Rubiño, and M. M. Pérez, "Gloss measurements and rugometric inspection in dental biomaterials," Proc. SPIE **8785** (2013).

[20] Y. Hosoya, T. Shiraishi, T. Odatsu, J. Nagafuji, M. Kotaku, M. Miyazaki, and J. M. Powers, "Effects of polishing on surface roughness, gloss, and color of resin composites," J. Oral Sci. **53**, no. 3, 283–291 (2011).

[21] R. Xu, P.D. Fleming, and A. Pekarovicova, "The effect of ink jet papers roughness on print gloss and ink film thickness," *Proc. IS&T's NIP20: Int'l Conf. on Digital Printing Technologies* (IS&T, Springfield, VA, 2004), pp. 439–444.

[22] M. C. Beland and J. M. Bennett, "Effect of local microroughness on the gloss uniformity of printed paper surfaces," J. Appl. Opt. **39**, 2719–2726 (2000).

[23] M. Juuti, T. Prykäri, E. Alarousu, H. Koivula, M. Myllys, A. Lähteelä, M. Toivakka, J. Timonen, R. Myllylä, and K. E. Peiponen, "Detection of local specular gloss and surface roughness from black prints," Colloids Surf. A **299**, 101–108 (2007).

[24] W. A. P. Smith and E. R. Hancock, "Specular and diffuse reflectance in microfacet models," *Proc. 16th IEEE Int'l. Conf. on Image Processing (ICIP)* (IEEE, Piscataway, NJ, 2009), pp. 3737–3740.

[25] C. Kelemen, L. Szirmay-Kalos, and L. Szirmay-kalos, "Microfacet based coupled specular-matte BRDF model with importance sampling," Eurograph. Conf. **25–34**, (2001).

[26] K. Baba, S. Inoue, R. Takano, and N. Tsumura, "Reproducing gloss unevenness on printed paper based on the measurement and analysis of mesoscopic facets," J. Imaging Sci. Technol. **58**, 030501 (2014).

[27] D. Benavente, F. Martínez-Verdú, A. Bernabeu, V. Viqueira, R. Fort, M. García del Cura, C. Illueca, and S. Ordóñez, "Influence of surface roughness on color changes in building stones color," Res. Appl. **28**, 343–351 (2003).

[28] V. Briones, J. M. Aguilera, and C. Brown, "Effect of surface topography on color and gloss of chocolate samples," J. Food Eng. **77**, 776–783 (2006).

[29] W. Matusik, B. Ajdin, J. Gu, J. Lawrence, H. P. Lensch, F. Pellacini, and S. Rusinkiewicz, "Printing spatially-varying reflectance," ACM Trans. Graph. **28**, 128 (2009).

[30] T. Malzbender, R. Samadani, S. Scher, A. Crume, D. Dunn, and J. Davis, "Printing reflectance functions," ACM Trans. Graph. **31**, 20 (2012).

[31] S. G. Wang, C. H. Liu, B. Xu, R. Eschbach, and G. G. Marcu, "Glossmark technology: beyond halftone frequencies," Proc. SPIE **5667**, 544–553 (2004).

[32] T. Weyrich, P. Peers, W. Matusik, and S. Rusinkiewicz, "Fabricating microgeometry for custom surface reflectance," ACM Trans. Graph. **28**, 31 (2009).

[33] M. Alexa and W. Matusik, "Reliefs as images," ACM Trans. Graph. **29**, 60 (2010).

[34] O. Rouiller, B. Bickel, J. Kautz, W. Matusik, and M. Alexa, "3D-printing spatially varying BRDFs," Comput. Graph. Appl. **33**, 48–57 (2013).

[35] Y. Lan, Y. Dong, F. Pellacini, and X. Tong, "Bi-scale appearance fabrication," ACM Trans. Graph. **32**, 145 (2013).

[36] T. Baar, S. Samadzadegan, H. Brettel, P. Urban, and M. Ortiz-Segovia, "Printing gloss effects in a 2.5D system," Proc. SPIE **9018**, 90180M (2014).

[37] T. Baar, H. Brettel, and M. Ortiz-Segovia, "Towards gloss control in fine art reproduction," Proc. SPIE **9398**, 29 (2015).

[38] H. Faken, "Inkjet printer and a method of printing a receiving material," US Patent 6,869,174 (2005).

[39] T. Baar, M. Ortiz-Segovia, and H. Brettel, "Colour management of prints with variant gloss," *Proc. IS&T's CIC22: Twenty-second Color and Imaging Conf.* (IS&T, Springfield, VA, 2014), pp. 48–52.

[40] ASME B46.1 2009 Surface Texture (Surface Roughness, Waviness, and Lay) (ASME, New York) www.asme.org .

[41] R. W. Fleming, R. O. Dror, and E. H. Adelson, "Real-world illumination and the perception of surface reflectance properties," J. Vis. **3**, 347–368 (2003).

[42] M. Giesel and K. R. Gegenfurtner, "Color appearance of real objects varying in material, hue, and shape," J. Vis. **10**, 10 (2010).

[43] Y. X. Ho, M. S. Landy, and L. T. Maloney, "Conjoint measurement of gloss and surface texture," J. Psychol. Sci. **19**, 196–204 (2008).

[44] G. Obein, K. Knoblauch, and F. Viénot, "Difference scaling of gloss: nonlinearity, binocularity, and constancy," J. Vis. **4**, 711–720 (2004).

[45] F. B. Leloup, P. Hanselaer, M. R. Pointer, and P. Dutré, "Integration of multiple cues for visual gloss evaluation," *Proc. Predicting Perceptions: the 3rd Int'l. Conf. on Appearance* (2012), pp. 52–55.

[46] S. Samadzadegan, T. Baar, P. Urban, M. Ortiz-Segovia, and J. Blahová, "Controlling colour-printed gloss by varnish-halftones," Proc. SPIE **9398**, 31 (2015).

[47] J. Wills, S. Agarwal, D. Kriegman, and S. Belongie, "Toward a perceptual space for gloss," ACM Trans. Graph. **28**, 103 (2009).

[48] T. Pereira and S. Rusinkiewicz, "Gamut mapping spatially varying reflectance with an improved BRDF similarity metric," *Proc. Eurographics Symposium on Rendering: Computer Graphics Forum* (2012), Vol. 31, pp. 1–10.

[49] A. Fores, M. D. Fairchild, and I. Tastl, "Improving the perceptual uniformity of a gloss space," *Proc. IS&T's CIC22: Twenty-second Color and Imaging Conf.* (IS&T, Springfield, VA, 2014), pp. 7–13.

[50] M. Oren and S. K. Nayar, "Generalization of Lambert's reflectance model," *Proc. 21st Annual Conf. on Computer Graphics and Interactive Techniques* (1994), 239–246.

[51] M. M. Bagher, C. Soler, and N. Holzschuch, "Accurate fitting of measured reflectances using a shifted gamma micro-facet distribution," *Comput. Graph. Forum 31* (John Wiley & Sons, Inc., 2012), pp. 1509–1518.

[52] B. Walter, S. R. Marschner, H. Li, and K. E. Torrance, "Microfacet models for refraction through rough surfaces," Proc. EGSR **2007**, (2007).

[53] S. Farnand and L. Ye, "The effects of color on gloss appearance and measurement," *Proc. IS&T's NIP23: Int'l Conf. on Digital Printing Technologies and Digital Fabrication 2007* (IS&T, Springfield, VA, 2007), pp. 373–377.